Packet Loss Rate Analysis of Wireless Sensor Transmission with RF Energy Harvesting

Tian-Qing Wu and Hong-Chuan Yang(✉)

Department of Electrical and Computer Engineering,
University of Victoria, Victoria, Canada
{twu,hy}@uvic.ca

Abstract. RF energy harvesting is a promising potential solution for providing convenient and perpetual energy supply to low-power wireless sensor networks. In this paper, we investigate the performance of overlaid wireless sensor transmission powered by RF energy harvesting from existing wireless system for delay sensitive traffic. We derive the exact closed-form expression for the distribution function of harvested energy over a certain number of coherence time over Rayleigh fading channels with the consideration of hardware limitation, such as energy harvesting sensitivity and efficiency. We further analyze the packet loss probability of sensor transmission subject to interference from existing system.

Keywords: RF energy harvesting · Sensitivity · Wireless sensor transmission

1 Introduction

Wireless sensor networks (WSNs) are used in a wide range of applications, such as environment monitoring, surveillance, health care, intelligent buildings and battle field control [1]. The sensor nodes of WSN are usually powered by batteries with finite life time, which manifests as an important limiting factor to the functionality of WSN. Replacing or charging the batteries may either incur high costs for human labor or be impractical for certain application scenarios (e.g. applications that require sensors to be embedded into structures). Powering sensor nodes through ambient energy harvesting has therefore received a lot of attentions in both academia and industrial communities [2,3]. Various techniques have been developed to harvest energy from conventional ambient energy sources, such as solar power, wind power, thermoelectricity, and vibrational excitations [4–7].

RF energy is another promising candidate ambient energy source for powering sensor nodes. Recently, there has been a growing interest in RF energy harvesting due to the intensive deployment of cellular/WiFi wireless systems in addition to traditional radio/TV broadcasting systems [8]. It has been experimentally proved that RF energy harvesting is feasible from the hardware implementation viewpoint. In [9], the authors developed prototypes for devices that communicate with each other using ambient RF signals from TV/cellular systems as the

M. Weichold et al. (Eds.): CROWNCOM 2015, LNICST 156, pp. 620–630, 2015.
DOI: 10.1007/978-3-319-24540-9_51

only power source. In [10], the authors present the experimental performance (e.g., charging time of the sensor and received signal power at the sink) of RF energy harvesting using PowerCast energy harvesters [11]. Although these previous works have proved a visible future for the wireless application based on RF energy harvesting, most performance results are obtained through laboratory experiments. There is still a lack of effective theoretical models that can analytically predict the performance of WSNs powered by RF energy harvesting.

Previous literature on RF energy harvesting can be summarized as following. The fundamental performance limits of simultaneous wireless information and energy transfer systems over point-to-point link were studied in [12,13]. In [14], the authors consider a three-node multiple-input multiple-output (MIMO) wireless system, where one receiver harvests energy and another receiver decodes information from the signal transmitted by a common transmitter. A cognitive network that can harvest RF energy from the primary system is considered in [15]. The authors propose an optimal mode selection policy for sensor nodes to decide whether to transmit information or to harvest RF energy based on Markov modelling. In [16], the authors investigate mode switching between information decoding and energy harvesting, based on the instantaneous signal channel and interference condition over a point-to-point link. In most of these works, it is generally assumed that the channel gain remains constant during the whole energy harvesting circle, including obtaining channel state information, making decision accordingly, and then harvesting energy or decoding information. It worths to point out that wireless fading channels are in general time varying with channel coherence time in the order of milliseconds. The harvested energy over one channel coherence time may not be sufficient for channel estimation alone, not to mention information transmission/decoding.

With these observations in mind, we consider an overlaid sensor transmission scenario where a sensor-to-sink communication link operates in the coverage of an existing wireless system over the same frequency. We assume that the sink has a constant power source and that the sensor needs to harvest RF energy from the transmission of existing wireless system. Specifically, the sensor node can only harvest RF energy when its received signal power is larger than a certain sensitivity level [14]. As such, the existing system, being either cellular, WiFi or TV broadcasting systems, serves as the ambient source for sensor energy harvesting and as interference source during sensor transmission. Such an overlaid implementation strategy of RF-energy powered WSN has the potential to offer attractive and green solutions to a wide range of sensing applications, particularly in view of the increasingly severe spectrum scarcity. We consider delay sensitive traffic scenario, where the sensor needs to periodically transmit a new packet to the sink. We investigate the packet transmission performance of the sensor-to-sink link over Rayleigh fading wireless channels over multiple channel coherence time. The statistical distribution of the amount of energy that can be harvested over a fixed number of channel coherence time is derived with the consideration of harvesting sensitivity and efficiency. We study the packet loss probability of delay sensitive traffic, which is dependent on the amount of harvested energy as well as interference amount experienced during packet transmission. We also examine the effect of traffic intensity and the energy storage capacity at the sensor on the packet loss probability based on the exact analytical results. These analytical results will help determine what type of sensing applications that the proposed overlaid implementation strategy can effectively support.

The remainder of the paper is organized as follows. In Section 2, we introduce the system and channel model under consideration. The performance of the proposed sensing implementation for delay sensitive traffic is evaluated in Section 3. Concluding remarks are given in Section 4.

2 System and Channel Model

2.1 System Model

We consider the point-to-point packet transmission from a single-antenna wireless sensor to its sink over a flat Rayleigh fading channel. The sink and the sensor are deployed in the coverage area of an existing wireless system, which could be cellular, WiFi or TV broadcasting systems. We assume that the sensor can harvest RF energy from the transmitted signal of the existing system, and use it as its sole energy source for transmission, as illustrated in Fig. 1.

In the energy harvesting stage, the sensor harvests RF energy from the radio transmission of existing wireless systems over multiple channel coherence time. Typically, the sensor can harvest RF energy only when the received signal power is larger than a power threshold, denoted by P_{th} [14]. In general, P_{th} should be greater than the receiver sensitivity for information reception.

During the packet transmission stage, the sensor will transmit its collected information to the sink using harvested energy. We assume that the energy consumed for information collection is negligible compared with the energy used for transmission [17]. Then the energy that can be used for transmission is approximately equal to the harvested energy. Also note that the sensor transmission will suffer interference from the existing system in this stage, the effect of which will be further discussed in the following sections. Due to the low transmission power and short transmission duration, we ignore the interference that the sensor transmission may generate to the existing system.

2.2 Channel Model

We adopt a log-distance path loss plus Rayleigh block fading channel models for the operating environment [19] while ignoring the shadowing effect for the sake of presentation clarity. In particular, the channel gain between the BS and the sensor remains constant over one channel coherence time, denoted by T_c, and changes to an independent value afterwards. Let h_n denote the fading channel gain over the nth coherence time, where $h_n \in \mathcal{CN}(0, 1)$. For notational conciseness, we use α_n

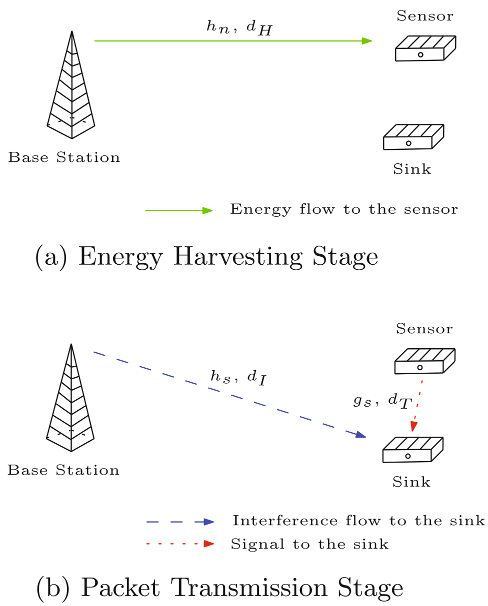

Fig. 1. System model for two-stage sensor transmission with RF energy harvesting.

to denote its amplitude square, i.e. $\alpha_n = ||h_n||^2$, whose PDF for Rayleigh fading channel under consideration is given by

$$f_{\alpha_n}(x) = e^{-x}. \tag{1}$$

Then the instantaneous received signal power at the sensor over the nth coherence time is given by $P_n = \overline{P}\alpha_n$, where $\overline{P}$ is the average received power at the sensor due to path loss, given by

$$\overline{P} = \frac{P_T}{\Gamma d_H^{\lambda}}, \tag{2}$$

where P_T is the constant transmission power of BS, d_H is the distance from BS to the sensor, λ is the path loss exponent of the environment, ranging from 2 to 5, and Γ is a constant parameter of the log-distance path loss model. Specifically, $\Gamma = \frac{PL(d_0)}{d_0^{\lambda}}$, where d_0 is a reference distance of the antenna far field, and $PL(d_0)$ is linear path loss at distance d_0, depending on the propagation environment.

We assume, as is the case in real world systems [10][11], the sensor can only harvest energy when the instantaneous received signal power P_n is greater than the sensitivity level P_{th} and the harvested energy is proportional to $P_n - P_{th}$. Consequently, the amount of energy that the sensor can harvest during the nth coherence time can be represented as [14]

$$E_n = \begin{cases} \eta T_c(P_n - P_{th}), & P_n \geq P_{th}; \\ 0, & P_n < P_{th}, \end{cases} \tag{3}$$

where $0 \leq \eta \leq 1$ is RF energy harvesting efficiency. It follows that the amount of energy harvested by the sensor over N consecutive coherence time can be given by

$$E_h^{(N)} = \min\left(\sum_{n=1}^{N} E_n, E_c\right), \tag{4}$$

where E_c is the energy storage capacity of the sensor. [1]

The transmission power of the sensor when it uses the harvested energy over N coherence time is equal to $\frac{E_h^{(N)}}{T_s}$, where T_s denotes the transmission time duration. We assume, with the notion of low-rate sensing applications, that T_s is much smaller than the channel coherence time T_c. Let h_s and g_s denote the fading channel gains from BS to the sink and from the sensor to the sink, respectively, where $h_s \in \mathcal{CN}(0,1)$ and $g_s \in \mathcal{CN}(0,1)$. The received SINR at the sink can be calculated as

$$\gamma_s = \frac{\frac{E_h^{(N)}}{T_s d_T^{\lambda}}||g_s||^2}{\frac{P_T}{d_I^{\lambda}}||h_s||^2 + \Gamma\sigma^2}, \tag{5}$$

where d_T is the distance from the sensor to the sink, d_I is the distance from BS to the sink, and σ^2 is the variance of the additive noise at the sink. In general, the sensor and the sink are very close to each other, i.e. $d_T \ll d_H \approx d_I$. In the following, we study the performance of such overlaid sensor transmission when it is used to support low-rate data traffics.

3 Performance Analysis for Delay Sensitive Traffic

For certain sensing applications, such as smart metering and environment monitoring, the sensor node needs to periodically send their collected information (e.g. energy usage, temperature, humid information) to the sink. Any delay in the delivery of these information may render them useless. Therefore, the goal is to successfully transmit these information packet within a fixed time duration. As such, an important performance metric for such application is the packet loss probability, i.e. the percent of packets that could not be delivered to the sink in time. We now analyze the packet loss probability of the proposed overlaid sensing implementation with RF energy harvesting. An accurate quantification of this metric will help determine the sensing applications that could be supported with the proposed implementation.

3.1 Distribution of Harvested Energy over N Coherence Time

We are interested in the distribution fuction of the harvested energy of the sensor over N channel coherence time, which will be used for packet loss probability analysis.

[1] E_c can also be viewed as the energy threshold, above which the sensor can carry out packet transmission.

We first consider the one coherence time case, i.e. $N = 1$. The CDF of the harvested energy can be simply represented as

$$F_{E_h^{(1)}}(x) = \Pr[E_h^{(1)} < x] = \Pr[E_1 < x], x \leq E_c. \tag{6}$$

After substituing (3) into (6) and some manipulation, we have

$$F_{E_h^{(1)}}(x) = 1 - e^{-\frac{x}{\eta T_c \overline{P}} - \frac{P_{th}}{\overline{P}}}, x \leq E_c. \tag{7}$$

For the multiple channel coherence time case, i.e. $N > 1$, we denote the number of channel coherence time, in which the sensor can harvest energy, by N_a. According to the total probability theorem, the CDF of the harvested energy is shown as

$$F_{E_h^{(N)}}(x) = \Pr[E_h^{(N)} < x] = \sum_{i=0}^{N} \Pr[\sum_{n=1}^{N} E_n < x, N_a = i]. \tag{8}$$

When the ith largest received power is larger than P_{th} and the $(i+1)$th largest one is lower than P_{th}, the number of coherence time that the sensor can harvest energy is $N_a = i$. We denote the ordered version of N i.i.d. random variables α_n as $\alpha_{1:N} \geq \alpha_{2:N} \geq \cdots \geq \alpha_{N:N}$, and the sum of the $i-1$ largest variables as $\beta_i = \sum_{j=1}^{i-1} \alpha_{j:N}$. We can show that $N_a = i$ if and only if $\alpha_{i:N} \geq \frac{\Gamma d_H^\lambda P_{th}}{P_T}$ and $\alpha_{i+1:N} < \frac{\Gamma d_H^\lambda P_{th}}{P_T}$. Therefore, $F_{E_h}(x)$ can be calculated as,

$$\begin{aligned} F_{E_h^{(N)}}(x) = & \sum_{i=2}^{N-1} \Pr[\beta_i + \alpha_{i:N} < \frac{x}{\eta T_c \overline{P}} + \frac{iP_{th}}{\overline{P}}, \alpha_{i:N} \geq \frac{P_{th}}{\overline{P}}, \alpha_{i+1:N} < \frac{P_{th}}{\overline{P}}] \\ & + \Pr[\alpha_{1:N} < \frac{P_{th}}{\overline{P}}] + \Pr[\frac{P_{th}}{\overline{P}} \leq \alpha_{1:N} < \frac{x}{\eta T_c \overline{P}} + \frac{P_{th}}{\overline{P}}, \alpha_{2:N} < \frac{P_{th}}{\overline{P}}] \\ & + \Pr[\beta_N + \alpha_{N:N} < \frac{x}{\eta T_c \overline{P}} + \frac{NP_{th}}{\overline{P}}, \alpha_{N:N} \geq \frac{P_{th}}{\overline{P}}] \\ = & \sum_{i=2}^{N-1} \int_{\frac{P_{th}}{\overline{P}}}^{\frac{x}{i\eta T_c \overline{P}} + \frac{P_{th}}{\overline{P}}} \int_{(i-1)y}^{\frac{x}{\eta T_c \overline{P}} + \frac{iP_{th}}{\overline{P}} - y} \int_0^{\frac{P_{th}}{\overline{P}}} f_{\beta_i, \alpha_{i:N}, \alpha_{i+1:N}}(t, y, z) dt dy dz \\ & + \int_0^{\frac{P_{th}}{\overline{P}}} f_{\alpha_{1:N}}(t) dt + \int_0^{\frac{P_{th}}{\overline{P}}} \int_{\frac{P_{th}}{\overline{P}}}^{\frac{x}{\eta T_c \overline{P}} + \frac{P_{th}}{\overline{P}}} f_{\alpha_{1:N}, \alpha_{2:N}}(t, y) dt dy \\ & + \int_{\frac{P_{th}}{\overline{P}}}^{\frac{x}{N\eta T_c \overline{P}} + \frac{P_{th}}{\overline{P}}} \int_{(N-1)y}^{\frac{x}{\eta T_c \overline{P}} + \frac{NP_{th}}{\overline{P}} - y} f_{\beta_N, \alpha_{N:N}}(t, y) dt dy, \end{aligned} \tag{9}$$

where $f_{\alpha_{1:N}}(x, y)$, $f_{\alpha_{1:N}, \alpha_{2:N}}(x, y)$, $f_{\beta_N, \alpha_{N:N}}(x, y)$, and $f_{\beta_i, \alpha_{i:N}, \alpha_{i+1:N}}(x, y, z)$ are the marginal and joint PDFs of $\alpha_{i:N}$ and β_i, whose closed-form expression can be obtained in [18]. By properly substituting the closed-form expression of $f_{\alpha_{1:N}}(x, y)$, $f_{\alpha_{1:N}, \alpha_{2:N}}(x, y)$, $f_{\beta_N, \alpha_{N:N}}(x, y)$, and $f_{\beta_i, \alpha_{i:N}, \alpha_{i+1:N}}(x, y, z)$ into (9) and carrying out integration, the close form expression of the CDF of harvested energy is obtained as

$$F_{E_h^{(N)}}(x) = \begin{cases} \sum_{i=2}^{N} \frac{N!(1-e^{-\frac{P_{th}}{\overline{P}}})^{N-i} e^{-\frac{iP_{th}}{\overline{P}}}}{(i-1)!(i-2)!(N-i)!} \sum_{m=0}^{i-2} (1-i)^{i-2-m} \binom{i-2}{m} \sum_{j=0}^{m} \frac{m!}{(m-j)!} \\ \Big\{ (i-1)^{m-j} \sum_{k=0}^{i-2-j} \frac{(i-2-j)!}{(i-2-j-k)! i^{k+1}} \Big[(\frac{P_{th}}{\overline{P}})^{i-2-j-k} \\ -e^{-\frac{x}{\eta T_c \overline{P}}} (\frac{x}{i\eta T_c \overline{P}} + \frac{P_{th}}{\overline{P}})^{i-2-j-k} \Big] - e^{-\frac{x}{\eta T_c \overline{P}}} \sum_{s=0}^{m-j} (-1)^{m-j-s} \binom{m-j}{s} \\ (\frac{x}{\eta T_c \overline{P}} + \frac{iP_{th}}{\overline{P}})^{s} \frac{(\frac{x}{i\eta T_c \overline{P}} + \frac{P_{th}}{\overline{P}})^{i-1-j-s} - (\frac{P_{th}}{\overline{P}})^{i-1-j-s}}{i-1-j-s} \Big\} + (1-e^{-\frac{P_{th}}{\overline{P}}})^{N} \\ +N(1-e^{-\frac{P_{th}}{\overline{P}}})^{N-1} (e^{-\frac{P_{th}}{\overline{P}}} - e^{-\frac{x}{\eta T_c \overline{P}} - \frac{P_{th}}{\overline{P}}}), & x \le E_c; \\ 1, & x > E_c. \end{cases} \tag{10}$$

After taking derivative with respect to x, the PDF of $F_{E_h}(x)$ is derived and given as

$$f_{E_h^{(N)}}(x) = \begin{cases} \sum_{i=2}^{N} \frac{N!(1-e^{-\frac{P_{th}}{\overline{P}}})^{N-i} e^{-\frac{x}{\eta T_c \overline{P}} - \frac{iP_{th}}{\overline{P}}}}{(i-1)!(i-2)!(N-i)!} \sum_{m=0}^{i-2} (1-i)^{i-2-m} \binom{i-2}{m} \\ \sum_{j=0}^{m} \frac{m!}{(m-j)!} \Big\{ (i-1)^{m-j} \sum_{k=0}^{i-2-j} \frac{(i-2-j)!}{(i-2-j-k)! i^{k+1}} (\frac{x}{i\eta T_c \overline{P}} + \frac{P_{th}}{\overline{P}})^{i-2-j-k-1} \\ (\frac{x}{i\eta^2 T_c^2 \overline{P}^2} + \frac{P_{th}}{\eta T_c \overline{P}^2} - \frac{i-2-j-k}{i\eta T_c \overline{P}}) + \sum_{s=0}^{m-j} (-1)^{m-j-s} \binom{m-j}{s} \frac{i^s}{i-1-j-s} \\ \{ (\frac{x}{i\eta T_c \overline{P}} + \frac{P_{th}}{\overline{P}})^{i-2-j} (\frac{x}{i\eta^2 T_c^2 \overline{P}^2} + \frac{P_{th}}{\eta T_c \overline{P}^2} - \frac{i-1-j}{i\eta T_c \overline{P}}) \\ +(\frac{P_{th}}{\overline{P}})^{i-1-j-s} (\frac{x}{i\eta T_c \overline{P}} + \frac{P_{th}}{\overline{P}})^{s-1} (-\frac{x}{i\eta^2 T_c^2 \overline{P}^2} - \frac{P_{th}}{\eta T_c \overline{P}^2} + \frac{s}{i\eta T_c \overline{P}}) \} \Big\} \\ + \frac{N}{\eta T_c \overline{P}} (1-e^{-\frac{P_{th}}{\overline{P}}})^{N-1} e^{-\frac{x}{\eta T_c \overline{P}} - \frac{P_{th}}{\overline{P}}} + (1-e^{-\frac{P_{th}}{\overline{P}}})^{N} \delta(x) \\ + \big[1 - F_{E_h}(E_c)\big] \delta(x-E_c), & N > 1; \\ \frac{1}{\overline{P}\eta T_c} e^{-\frac{x}{\overline{P}\eta T_c} - \frac{P_{th}}{\overline{P}}} + (1-e^{-\frac{P_{th}}{\overline{P}}})^{N} \delta(x) + \big[1 - F_{E_h}(E_c)\big] \delta(x-E_c), & N = 1, \end{cases} \tag{11}$$

where $\delta(\cdot)$ denotes the impulse function. Note that the PDF involves two impulse function at 0 and E_c due to the capacity constraints.

3.2 Packet Loss Probability Analysis

We assume that the sensor must collect and transmit one packet to the sink over a fixed time duration T_F. The number of coherence time in T_F, denoted by N, is approximately equal to $\lfloor \frac{T_F}{T_c} \rfloor$. The sensor will first harvest RF energy for N channel coherence time and then transmit the packet to the sink using the harvested energy. We focus on low rate sensing application and ignore the potential packet collision with other sensors. We also assume that, with adoption of certain error correction coding scheme, the packet can be successfully received by the sink if the received SINR at the sink during packet transmission is above γ_T. As such, packet loss will occurs if and only if the received SINR at the sink during packet transmission is below the threshold γ_T. This may be due to insufficient harvested energy, poor sensor to sink channel quality, as well as strong interference from BS. Mathematically, the packet loss probability of the sensor transmission is given by

$$P_{PL} = \Pr[\gamma_s < \gamma_T] = \Pr[\frac{\frac{E_h^{(N)}}{T_s d_T^{\lambda}} ||g_s||^2}{\frac{P_T}{d_I^{\lambda}} ||h_s||^2 + \Gamma \sigma^2} < \gamma_T]. \tag{12}$$

Conditioning on $E_h^{(N)}$, the packet loss probability can rewritten in terms of the PDFs of $E_h^{(N)}$, $||g_s||^2$, and $||h_s||^2$, denoted by $f_{E_h^{(N)}}(\cdot)$, $f_{||g_s||^2}(\cdot)$, and $f_{||h_s||^2}(\cdot)$, respectively, as

$$P_{PL} = \int_0^{E_c} \int_0^{\infty} F_{||g_s||^2}\left(\frac{T_s \gamma_T d_T^{\lambda}(\frac{P_T y}{d_I^{\lambda}} + \Gamma\sigma^2)}{z}\right) f_{||h_s||^2}(y) f_{E_h^{(N)}}(z) dy dz. \quad (13)$$

The PDF of $||h_s||^2$ and $||g_s||^2$ for the Rayleigh fading channel model under consideration are commonly given by

$$f_{||h_s||^2}(x) = f_{||g_s||^2}(x) = e^{-x}. \quad (14)$$

After proper substitution and some manipulations, we can rewrite P_{PL} as

$$P_{PL} = \int_0^{E_c} \left(1 - \frac{z e^{-\frac{T_s \gamma_T \Gamma d_T^{\lambda} \sigma^2}{z}}}{z + \frac{P_T}{d_I^{\lambda}} T_s \gamma_T d_T^{\lambda}}\right) f_{E_h^{(N)}}(z) dz. \quad (15)$$

Finally, the packet loss probability for delay sensitive traffic can be calculated by substituting (11) into (15) and carrying out numerical integration. Note that only finite integration of some basic functions are involved in the calculation.

3.3 Numerical Results

We assume the same parameters for RF energy harvesting system as in [9]. In particular, the transmission power of BS is $P_T = 10kW$. The distance from BS to the sensor, BS to the sink and the sensor to the sink are set as $d_H = 100$ meters, $d_I = 100$ meters and $d_T = 1$ meter, respectively. The pass loss exponent λ is assumed to be 3, the channel coherence time T_c be $100ms$, and the transmission time of the sensor T_s be $1ms$. The sensitivity of the sensor is assumed to be $P_{th} = -10dBm = 0.1mW$ [10]. For simplicity, we assume harvesting efficiency $\eta = 1$ and packet loss constant $\Gamma = 1$.

In Fig. 2, we plot the PDF of harvested energy over $N = 1, 2, 3$ coherence time. We can see that $E_h^{(N)}$ follows a mixed distribution with impulse at $x = 0$ and $x = E_c$, which represents the probability that the sensor can not harvest any energy over N coherence time and the probability that the sensor will be fully charged after N coherence time. With the increase of the number of coherence time N, the continuous portion of probability mass moves towards right, with the distribution of harvested energy spreads more widely along the energy axis. This is because when N increases, the sensor has larger probability to harvest more energy.

In Fig. 3, we plot the packet loss probability at the sink as a function of the SINR threshold for different energy capacity E_c with $N = 3$. We can see when γ_T is small, the packet loss probability shows approximately linear degradation. We also observe that larger energy capacity E_c leads to smaller packet loss probability. However, the benefit of lowing packet loss probability shrinks with

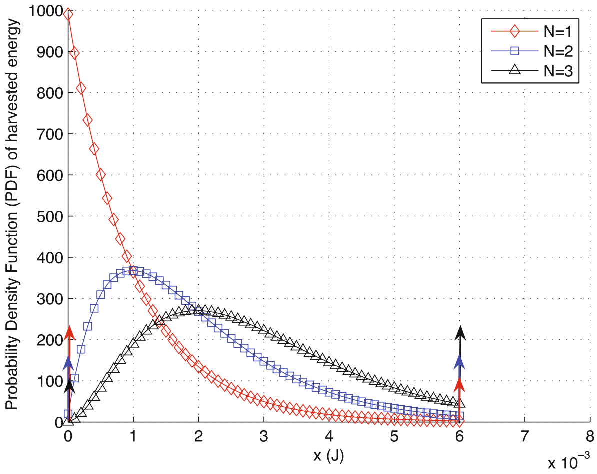

Fig. 2. Distribution of harvested energy over N channel coherence time ($E_c = 0.006J$).

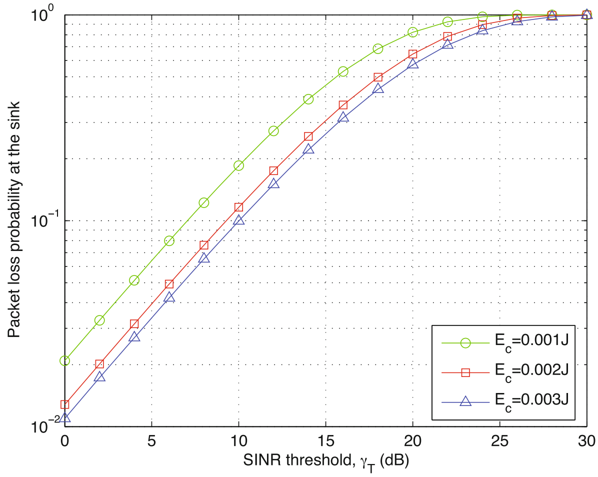

Fig. 3. Packet loss probability at the sink for different energy storage capacity.

the increase of the energy capacity E_c. This is because when E_c gets larger, the sensor has smaller probability to be fully charged, such that the effect of the energy capacity on the packet loss probability gradually reduces.

In Fig. 4, we plot the packet loss probability at the sink as a function of the number of the channel coherence time before each packet transmission. We can see the packet loss probability at the sink gradually reduces as N increases, and converge to a constant value when N is very large. This is due to the existence

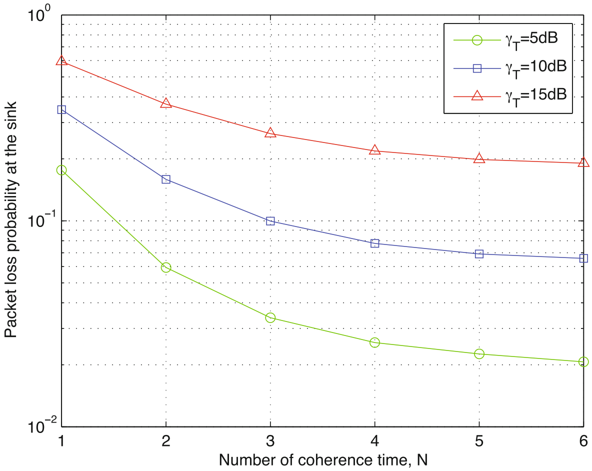

Fig. 4. Packet loss probability at the sink over N coherence time.

of energy storage capacity E_c, which limits the total harvested energy and in turn the transmission power. Moreover, we notice that higher SINR threshold leads to higher packet loss probability, as expected by intuition.

4 Conclusion

In this paper, we investigated the packet transmission performance of wireless sensor nodes powered through harvesting RF energy from existing wireless systems. We derive the exact closed-form expression for the distribution function of harvested energy over a certain number of coherence time over Rayleigh fading channels, based on which we further analyze the packet loss probability of sensor transmission with the consideration of hardware limitation, such as harvesting sensitivity and energy storage capacity, and interference from existing system. The analytical results will greatly facilitate the design and optimization of such sensor system powered by RF energy harvesting for the appropriate target sensing applications.

References

1. Akyildiz, I., Su, W., Sankarasubramaniam, Y., Cayirci, E.: A Survey on Sensor Networks. IEEE Communications Magazine **40**(8), 102–114 (2002)
2. Seah, W., Eu, Z.A., Tan, H.P.: Wireless sensor networks powered by ambient energy harvesting (wsn-heap) - survey and challenges. In: 1st International Conference on Wireless Communication, Vehicular Technology, Information Theory and Aerospace Electronic Systems Technology, Wireless VITAE 2009, pp. 1–5 (2009)
3. Sudevalayam, S., Kulkarni, P.: Energy Harvesting Sensor Nodes: Survey and Implications. IEEE Communications Surveys Tutorials **13**(3), 443–461 (2011)

4. Alippi, C., Galperti, C.: an Adaptive System for Optimal Solar Energy Harvesting in Wireless Sensor Network Nodes. IEEE Trans. on Circuits and Systems **55**(6), 1742–1750 (2008)
5. Weimer, M., Paing, T., Zane, R.: Remote area wind energy harvesting for low-power autonomous sensors. In: 37th IEEE Power Electronics Specialists Conference, pp. 1–5 (2006)
6. Mateu, L., Codrea, C., Lucas, N., Pollak, M., Spies, P.: Energy harvesting for wireless communication systems using thermogenerators. In: Proc. of the XXI Conference on Design of Circuits and Integrated Systems (DCIS), Barcelona, Spain (2006)
7. Tan, Y.K., Hoe, K.Y., Panda, S.K.: Energy harvesting using piezoelectric igniter for self-powered radio frequency (RF) wireless sensors. In: Proc. of IEEE Intel. Conference on Industrial Technology (ICIT), pp. 1711–1716 (2006)
8. Le, T., Mayaram, K., Fiez, T.: Efficient Far-field Radio Frequency Energy Harvesting for Passively Powered Sensor Networks. IEEE Journal of Solid-State Circuits **43**(5), 1287–1302 (2008)
9. Liu, V., Parks, A., Talla, V., Gollakota, S., Wetherall, D., Smith, J.R.: Ambient backscatter: wireless communication out of thin air. In: Proc. ACM SIGCOMM, pp. 1–13 (2013)
10. Baroudi, U., Qureshi, A., Talla, V., Gollakota, S., Mekid, S., Bouhraoua, A.: Radio frequency energy harvesting characterization: an experimental study. In Proc. IEEE TSPCC, pp. 1976–1981 (2012)
11. Powercast Corporation. http://www.powercastco.com
12. Varshney, L.R.: Transporting information and energy simultaneously. In: Proc. IEEE Int. Symp. Inf. Theory (ISIT), pp. 1612–1616 (2008)
13. Grover, P., Sahai, A.: Shannon meets tesla: wireless information and power transfer. In: Proc. IEEE Int. Symp. Inf. Theory (ISIT), pp. 2363–2367 (2010)
14. Zhang, R., Ho, C.K.: MIMO Broadcasting for Simultaneous Wireless Information and Power Transfer. IEEE Trans. Wireless Commun. **12**(5), 1989–2001 (2013)
15. Park, S., Heo, J., Kim, B., Chung, W., Wang, H., Hong, D.: Optimal mode selection for cognitive radio sensor networks with RF energy harvesting. In: Proc. IEEE PIMRC, pp. 2155–2159 (2012)
16. Liu, L., Zhang, R., Chua, K.: Wireless Information Transfer with Opportunistic Energy Harvesting. IEEE Trans. Wireless Commun. **12**(1), 288–300 (2013)
17. Raghunathan, V., Ganeriwal, S., Srivastava, M.: Emerging Techniques for Long Lived Wireless Sensor Networks. IEEE Commun. Mag. **44**(4), 108–114 (2006)
18. Yang, H.C., Alouini, M.S.: Order Statistics in Wireless Communications. Cambridge University Press (2011)
19. Goldsmith, A.: Wireless Communications. Cambridge University Press (2005)